Journal of Zhejiang University SCIENCE A
ISSN 1673-565X (Print); ISSN 1862-1775 (Online)
www.zju.edu.cn/jzus; www.springerlink.com
E-mail: jzus@zju.edu.cn

A gravity heat pipe for high voltage vacuum interrupter*

Xiao-ling YU[1], Zhi-yuan LIU[2], Quan-ke FENG[1], Yi-jiang WEI[1], Ji-mei WANG[2], Xiang-jun ZENG[†‡2]

([1]*School of Energy and Power Engineering, Xi'an Jiaotong University, Xi'an 710049, China*)

([2]*School of Electrical Engineering, Xi'an Jiaotong University, Xi'an 710049, China*)

[†]E-mail: zengxj@mail.xjtu.edu.cn

Received Apr. 8, 2008; Revision accepted Aug. 10, 2008; Crosschecked Aug. 20, 2009

Abstract: To enhance nominal current of high voltage vacuum circuit breakers (VCBs), a gravity heat pipe was proposed to replace stationary conducting rod of a high voltage vacuum interrupter. The heat pipe is composed of two coaxis tubes: the external tube is made of oxygen-free copper and the inner tube is made of stainless steel. The bottom end of the inner stainless steel tube is connected to the external copper tube by holes. Transient and static thermal performance of the heat pipe was measured, and the thermal resistance of it was compared with that of a solid copper rod with the same dimensions. Experimental results showed that thermal resistance of the heat pipe was about 1/3 of that of the copper rod, and it decreased slightly with the rising of the input heat flux. 3D thermal simulation on a 126 kV/2000 A single break VCB was done to compare the thermal performance between the proposed gravity heat pipe and the copper rod serving as the stationary conducting rod of the vacuum interrupter. Simulation results revealed that in the heat pipe case, the maximum temperature between contacts was 67 °C lower than that in the copper rod case.

Key words: Heat pipe, Vacuum circuit breakers (VCBs), Vacuum interrupters, Nominal current, Thermal simulation
doi:10.1631/jzus.A0820724 **Document code:** A **CLC number:** TM561.2

INTRODUCTION

Recently, the development of high voltage (≥72 kV) vacuum circuit breakers (VCBs) has drawn international interests in circuit breaker community (Matsui *et al*., 2005; Okubo, 2006; Renz, 2006; Yanabu, 2006; Liu *et al*., 2007), due to high global warming effect of SF_6 gas, which was specified in Kyoto conference in 1997. However, it is difficult to increase nominal current level of high voltage VCBs because the only effective heat transfer approach is heat conduction and heat radiation in vacuum interrupters. Heat convection does not help. So technologies to increase nominal current of high voltage VCBs have become a common interest in the field. It is well known that approaches to increase nominal current of a VCB include increase of diameters of conducting rods and other current carrying conductors, and reduction length of conduction path and installment of heat radiators.

In addition, various technologies were proposed. Matsukawa *et al*.(1998; 2000) developed a water-cooled VCB and found that a continuous current of 18 kA would be possible in the VCB, and also developed a forced-air cooling VCB. This technology enabled the nominal current of the VCB to reach 12 kA (8 kA in case of natural-air cooling). Fink *et al*.(2003) developed a new contact material based on a multilayer system, which had higher thermal and electrical conductivity, thus the contact resistance was reduced and the nominal current was increased.

Besides the above-mentioned high efficiency methods, heat pipe is a new approach to increase nominal current of a VCB because of its high effective thermal conductivity. It is widely used in the field of personal computers (Xie *et al*., 1998), integrated power electronic modules (IPEMs) (Martens *et al*., 2005), avionics (Zaghdoudi and Teytu, 2000), and many power electronics devices. Recently, heat pipes were reported to be utilized in the vacuum interrupter (Yamano *et al*., 2002), where a heat pipe was installed

‡ Corresponding author

* Project (No. 200806981005) supported by the New Teacher Foundation of MOE, China

in the stationary conducting rod. Temperature rise measurement showed that the maximum temperature was between a pair of contacts. It reached to 130 °C for the heat pipe installed case at 2000 A for 120 min, while it was 185 °C for the solid copper rod case.

In previous studies, the heat pipe was inserted in the stationary conducting rod (Yamano *et al*., 2002). So there was interference thermal resistance between the heat pipe and the stationary conducting rod of the vacuum interrupter. In our study, the stationary conducting rod was actually replaced by a gravity heat pipe. We studied its transient and static thermal performances, and compared it with a copper rod with the same size. At last, we simulated the temperature distribution of a 126 kV vacuum interrupter respectively when the stationary conducting rod was the copper rod and the heat pipe.

EXPERIMENT

Heat pipe structure and principle

Fig.1 shows the structure of the gravity heat pipe. The heat pipe was a coaxial tube. The external tube was made of oxygen-free copper and the inner tube was made of stainless steel. The bottom end of the inner stainless steel tube was connected to the external copper tube by 4 holes with diameters of 12 mm. The heat pipe was vacuumed. When the vacuum degree in the coaxial tube reached to 1×10^{-2} Pa, the de-ionized water was filled into and the cap was sealed. For a gravity heat pipe, the best filling ratio is about 18%~20% (Feldman and Srinivasan, 1984). We set the filling ratio as 19%. Considering water attached on walls, the actual filling ratio was about 17%. The heat pipe is assumed to be installed vertically to the ground as in the case of a live-type high voltage VCB. The de-ionized water is vaporized by ohmic heat from the contacts located at the bottom end of the heat pipe. The vapor flows up to the condensed region through the inner stainless steel tube, and condensed on the inner wall of the external copper tube by heat radiators. The condensed water flows back to the bottom end of the heat pipe along the inner wall of external copper tube because of its gravity. Therefore, heat generated from the contacts is transferred out by cycles of vaporizing and condensing of the de-ionized water.

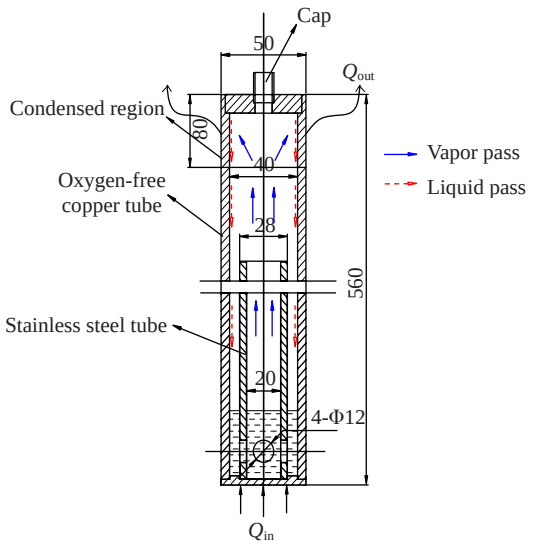

Fig.1 Structure of the gravity heat pipe. The vapor flows up along the inner stainless steel tube and the condensed water flows down along inner wall of the external copper tube. Heat generated from the contacts is transferred out by cycles of vaporizing and condensing of the de-ionized water. Q_{in} and Q_{out} are input heat flux and output heat flux, respectively (unit: mm)

Temperature measurement

In high voltage VCBs, the maximum temperature rise locates in the interface between a pair of contacts. The contacts are the most significant heat source in VCBs. To simulate this situation, Fig.2 shows the experimental setup. In the experiments, ohmic heat of the contacts was simulated by an electric heating plate positioned at the bottom of the heat pipe. The electric heating power, which was measured by a watt-meter (HIOKI 3286), was controlled between 100 to 200 W by a transformer to simulate heat of contacts in a 126-kV single break VCB with nominal current around 2000 A. In the upper part of external copper tube, there was a condensed region (length of 80 mm in Fig.1), under which the external copper tube was covered by asbestos used as an adiabatic envelope to simulate thermal insulation in vacuum. Forced air cooling by a fan was used to cool the condensed region. The wind velocity was about 2 m/s in a wind tunnel. We used 12 copper-constantan thermal couples to measure temperature distribution along the heat pipe, as shown in Fig.2b. The measuring point 1 was positioned at the bottom of the heat pipe. The measuring points 2 and 3 were positioned

under the liquid level. The measuring points 4 to 9 were positioned uniformly in the thermal insulation region. These 9 measuring points were covered by asbestos. The measuring points 10, 11, and 12 were arranged uniformly along the length of the condensed region. The temperatures were recorded with a 2-s interval by a temperature monitoring instrument. The ambient temperature was 20 °C.

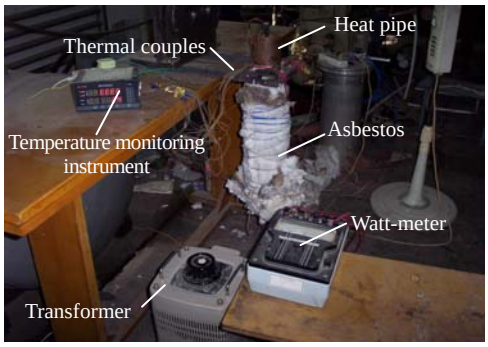

(a)

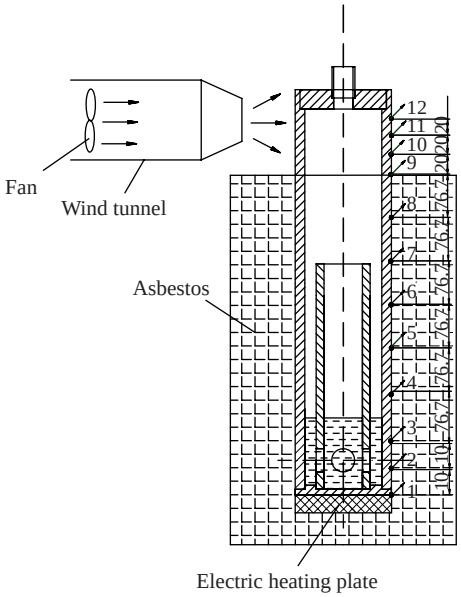

(b)

Fig.2 Experiment setup. (a) Photo of experiment setup; (b) Arrangements of temperature measuring points 1~12. Points 1~3 were under the liquid level, points 4~9 were in the thermal insulation region and points 10~12 were in the condensed region (unit: mm)

RESULTS

Transient thermal performance of the heat pipe

Fig.3 shows the transient temperature distribution of the heat pipe when the electric heating power was 200 W. It can be seen that the temperatures increased rapidly before 125 min. After 150 min, the heat pipe worked at a static state.

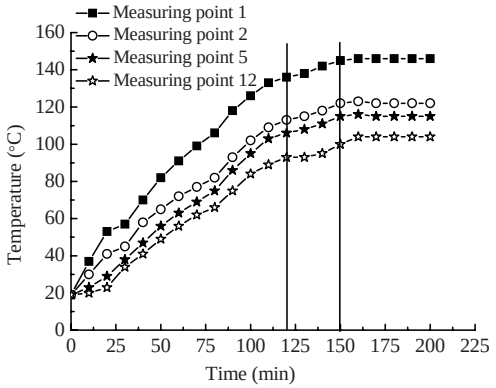

Fig.3 Transient temperature characteristics of the heat pipe. The locations of 1, 2, 5 and 12 can be referred to Fig.2. The ambient temperature was 20 °C

Static temperature distribution along the heat pipe

Fig.4 shows the static temperature distribution along the heat pipe at various heating power. Note that the temperature difference between the measuring points 1 and 2 was much higher than those between remain measuring points. This is because there was thermal resistance between the base of the heat pipe and the body of heat pipe due to welding. The temperature distribution from points 4 to 9 was almost flat. This is because almost all of heat was taken away by the water vapor flowing up from the bottom to the upper part of the heat pipe under very small pressure difference and temperature difference.

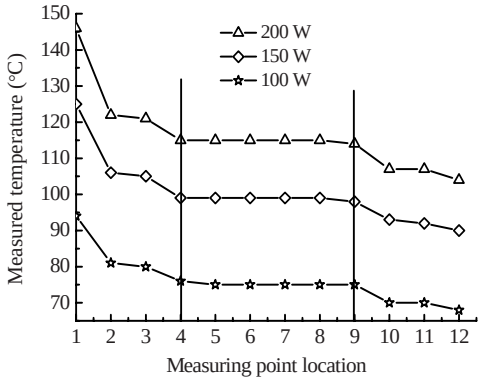

Fig.4 Static temperature distribution along the heat pipe. The ambient temperature was 20 °C

Thermal resistance comparison between the heat pipe and a solid copper rod

We compared the thermal resistances of the heat pipe and that of a solid copper rod with the same dimension. The heat transfer process in the copper rod is shown in Fig.5a. It can be simplified as a 1D thermal conduction problem because the heat flux on the bottom is uniform, and moreover, the dimension in length of the rod is much larger than that in diameter. Therefore, as shown in Fig.5b, the temperature of each point at the copper rod corresponding to each measuring point at the heat pipe can be calculated by solving the 1D thermal conduction equation as Eq.(1a). In the solving process, we assumed that boundary conditions of the copper rod, as shown in Eqs.(1b) and (1c), were the same as those of the heat pipe. Therefore, the temperature of point 12 at the copper rod was equal to that at the heat pipe.

$$\frac{\mathrm{d}^2T}{\mathrm{d}x^2}=0, \tag{1a}$$

$$-\lambda F\left.\frac{\partial T}{\partial x}\right|_{x=0}=Q_{\mathrm{in}}, \tag{1b}$$

$$T\big|_{\text{12-copper-rod}}=T_{\text{12-heat-pipe}}, \tag{1c}$$

where λ is thermal conductivity of the copper, W/(m·K); F is cross-sectional area of the copper rod, m^2; Q_{in} is the heating power, W. Q_{in} is equal to Q_{out} at the thermal static state.

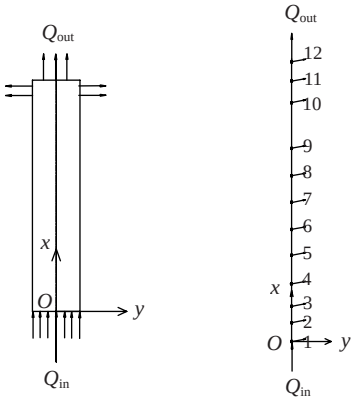

(a) (b)

Fig.5 Thermal conduction along the copper rod. (a) Heat transfer process; (b) 1D thermal conduction mode. In a stationary conducting rod of a live-type high voltage VCB, the heat transferred from one end to the other end of the copper rod

In Fig.6, we compared the measured temperature distribution on the heat pipe and the calculated temperature distribution on the copper rod when the heating power was 200 W. Note that the temperature gradient along the copper rod was much higher than that of the heat pipe. The temperature of point 1 at the copper rod was 93 °C higher than that at the heat pipe. The thermal resistance of the heat pipe is calculated according to

$$R_{\mathrm{hp}}=\frac{\Delta T}{Q}, \tag{2}$$

where R_{hp} is thermal resistance of the heat pipe, °C/W; and ΔT is temperature difference of the two ends of the heat pipe, °C.

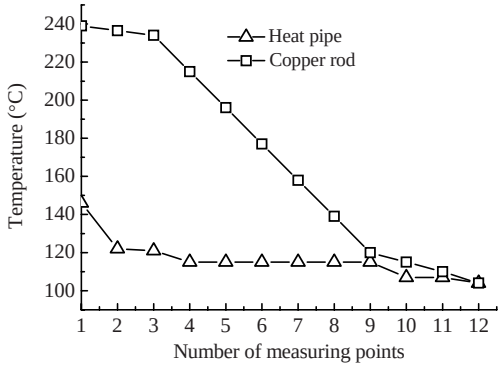

Fig.6 Measured temperature distribution along the heat pipe and calculated temperature distribution along the copper rod. The electric heating power was 200 W

The thermal resistance of the copper rod can be calculated according to

$$R_{\mathrm{cr}}=\frac{l}{\lambda F}, \tag{3}$$

where l is the length of the copper rod, m.

Thermal resistance of the heat pipe at various electric heating powers and that of the copper rod are shown in Fig.7. Note that thermal resistance of the heat pipe decreased slightly with the increasing of electric heating power. This was due to the boiling and condensing heat transfer coefficients increasing with the heat flux. Thermal resistance of the copper rod was 0.7 °C/W. It was about three times of thermal resistance of the heat pipe.

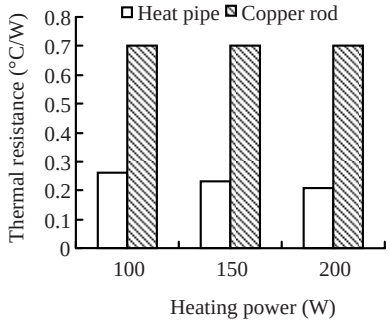

Fig.7 Thermal resistances of the heat pipe and the copper rod. The heat pipe and the copper rod have the same dimensions

THERMAL SIMULATION

As mentioned above, the gravity heat pipe had higher heat transfer performance than the solid copper rod. We did thermal simulation on a 126-kV single break VCB (Wang, 2006; Liu *et al.*, 2007) to compare temperature rise of the two cases. The stationary conducting rod of vacuum interrupter is either the solid copper rod or the gravity heat pipe. The rated current of the 126-kV VCB is 2000 A.

Internal structure of the conducting path of the 126-kV VCB is shown in Fig.8. Electrical current flows into the VCB from terminal 1, and flows out from terminal 2. Two heat radiators were used. The heat radiator structure is shown in Fig.9.

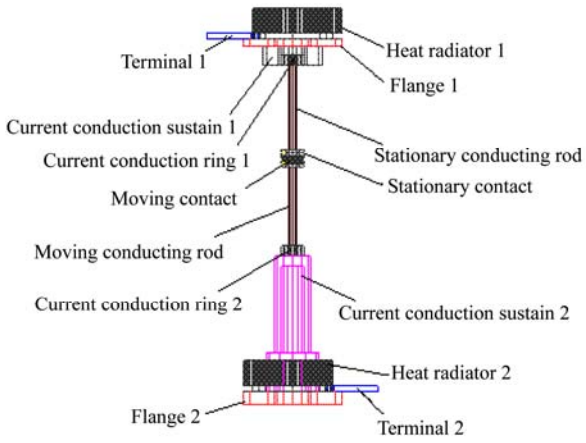

Fig.8 Cross section of the conducting path of a 126-kV VCB with nominal rated current 2000 A

Fig.9 Structure of the heat radiator. Structure of the heat radiators 1 and 2 were the same

To determine the boundary conditions, we calculated general heat transfer coefficients including natural convection and heat radiation on surfaces of the heat radiator and on other surfaces exposed in the air by a commercial computational fluid dynamic software. The computation domain of the heat radiator is illustrated in Fig.10, which includes the zone between two neighbor fins' center sections because fins were symmetrical distributed on the heat radiator base. Two side faces of the computation domain were respectively central planes of two neighbor fins. Height of the computation domain was 5 times of the fin height. The ambient temperature was set at 10 °C. Temperature of the heat radiator base was set at 40 °C. The calculated general heat transfer coefficients on the fins surface, heat radiator base surface and terminal surface are 7.74, 2.26, and 9.25 W/(m^2·K), respectively. Surfaces of the stationary conducting rod and the moving conducting rod are adiabatic for they are in a vacuum enclosure.

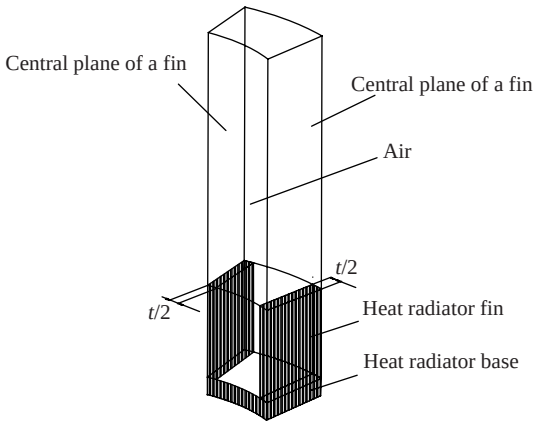

Fig.10 Computation domain of the heat radiator. Two side faces of the computation domain were respectively central planes of two neighbor fins. Height of the computation domain was 5 times of the fin height. *t* is thickness of heat radiator fin, the ambient temperature was 10 °C, temperature of the heat radiator base was 40 °C

The thermal simulation results of two cases in the 126-kV VCB are compared in Fig.11. The highest temperature at the contact is 317 °C in case of solid copper rod, while it is 250 °C in case of gravity heat pipe. So the highest temperature is decreased by 67 °C when the gravity heat pipe is used as the stationary conducting rod.

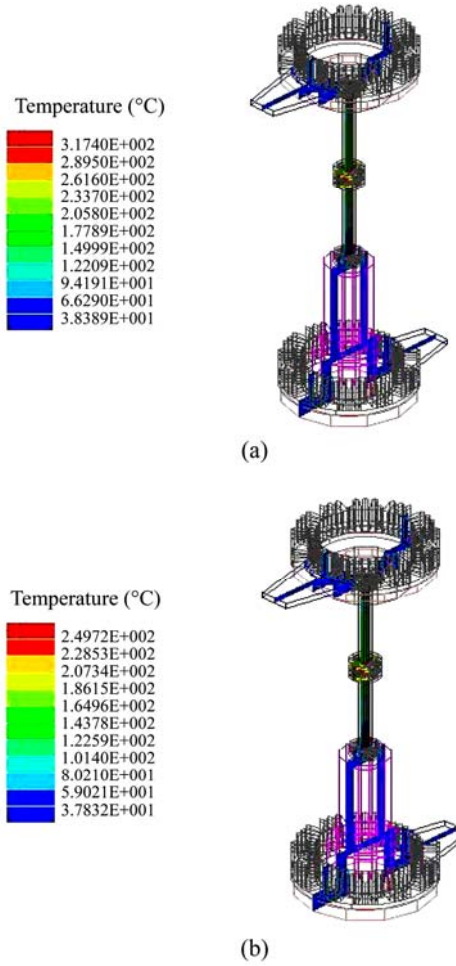

Fig.11 Simulated temperature distribution in a 126-kV VCB with nominal current 2000 A. The ambient temperature was 10 °C. Stationary conducting rod is (a) solid copper rod; (b) heat pipe

DISCUSSION

Thermal circuit of the vacuum interrupter

Thermal circuit from the stationary contact to ambient in case of solid copper rod in the 126-kV VCB is shown in Fig.12. T_a, $T_{hr1\text{-}b}$, $T_{sr\text{-}up}$, $T_{sr\text{-}low}$, T_{cont} are temperatures of the ambient, bottom of the heat radiator 1, upper end of the stationary conducting rod, lower end of the stationary conducting rod, and the stationary contact (Fig.8), respectively. $R_{hr1\text{-}a}$, $R_{sr\text{-}hr1}$, R_{sr}, $R_{cont\text{-}sr}$ are thermal resistances of the heat radiator 1 to ambient, upper end of the stationary conducting rod to the heat radiator 1, the stationary conducting rod, and lower end of the stationary conducting rod to the stationary contact, respectively. Q is the heat transferred from the stationary contact to the ambient. The thermal resistances were calculated as Eq.(2). The temperatures (Fig.11a) and the thermal resistances are shown in Table 1.

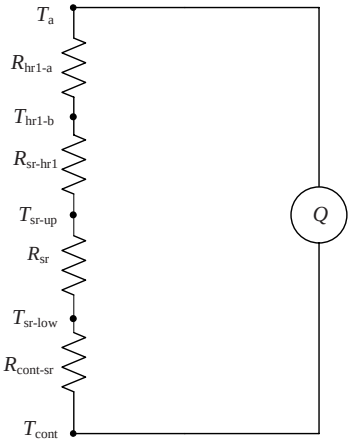

Fig.12 Thermal circuit from the stationary contact to the ambient in a 126-kV VCB with nominal current of 2000 A. The ambient temperature was 10 °C, stationary conducting rod is solid copper rod. The simulated temperature distribution is shown in Fig.11a

Table 1 Temperatures and thermal resistances in the thermal circuit

Temperature (°C)	Value	Thermal resistance (K/W)	Value
T_{cont}	317	$R_{cont\text{-}sr}$	142/Q
$T_{sr\text{-}low}$	175	R_{sr}	93/Q
$T_{sr\text{-}up}$	82	$R_{sr\text{-}hr1}$	39/Q
$T_{hr1\text{-}b}$	43	$R_{hr1\text{-}a}$	33/Q
T_a	10		

From Table 1, we see that the highest thermal resistance is $R_{cont\text{-}sr}$, which depends on the structure of the stationary contact. In order to reduce $R_{cont\text{-}sr}$, a balance between thermal performance and high current interruption performance, i.e., magnetic field and mechanical performance should be considered in electrode design. But it is a topic out of scope of this study. The second high is R_{sr}, which depends on di-

ameter and length of the stationary conducting rod. The objective of using the heat pipe is to reduce R_{sr}.

Inner diameter of the heat pipe

Thermal performance of the heat pipe is affected by its inner diameter because the vapor area has important effect on the heat pipe performance. Thermal performance of the heat pipe improves with increasing of the inner diameter, because high thermal conductivity of the heat pipe depends on the vapor space. However, the ohmic heat of the heat pipe also rises with increasing of the inner diameter because electric resistance of the heat pipe increases. Fig.13 shows the ohmic heat of the heat pipe (Fig.1) changing with its inner diameter. We find that the ohmic heat rises slightly with the inner diameter increasing up to 40 mm, and it rises quickly when the inner diameter is over 40 mm. Therefore, in design of the heat pipe, both the thermal performance and its ohmic heat should be considered, and the inner diameter of the heat pipe should be optimized.

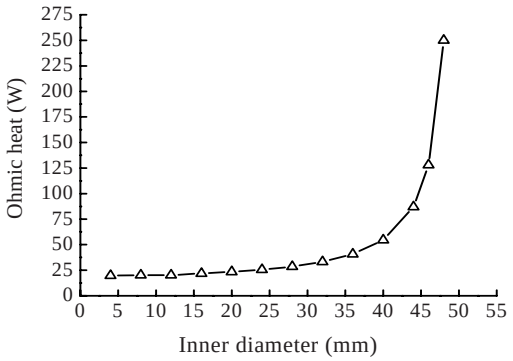

Fig.13 Ohmic heat of heat pipe changing with its inner diameter. The heat pipe is shown in Fig.1. The nominal current is 2000 A

CONCLUSION

We measured transient and static thermal performances of the gravity heat pipe serving as a stationary conducting rod of a high voltage vacuum interrupter. Thermal resistance of the heat pipe was compared with that of a solid copper rod with the same dimension. We can draw conclusions below:

(1) Temperature gradient on the body of the heat pipe was much lower than that of the solid copper rod.

(2) Thermal resistance of the heat pipe was about 1/3 of that of the solid copper rod in our experimental condition. The thermal resistance of the heat pipe decreased slightly with the increasing of input heat flux.

(3) Thermal simulation results showed that the highest temperature at the interface of a pair of contacts reduced by 67 °C when the gravity heat pipe was used to replace the solid copper rod which was usually used as a stationary conducting rod of the 126-kV single break VCB with nominal current of 2000 A.

Although the gravity heat pipe is promising to be used in high voltage VCBs, there are still problems to be solved. First, structure of the heat pipe should be optimized to enhance thermal performance and simultaneously it should meet mechanical strength requirements. The start-up problem of the gravity heat pipe should be further studied. Also, high electric current flows in the wall of the heat pipe when it is used in high voltage VCBs. Now we do not know whether or not the working condition in the high voltage VCB influences the life and reliability of the heat pipe. These problems should be studied in future work.

References

Feldman, J., Srinivasan, R., 1984. Investigation of Heat Transfer Limits in Two-phase Closed Thermosyphon. Proceedings of 5th International Heat Pipe Conference, Tsukuba, Japan.

Fink, H., Gentsch, D., Heimbach, M., 2003. Multilayer contact material based on copper and chromium material and its interruption ability. *IEEE Transaction on Plasma Science*, **31**(5):973-976. [doi:10.1109/TPS.2003.818425]

Liu, Z., Wang, J., Xiu, S., Wang, Z., Yuan, S., Jin, L., Zhou, H., Yang, R., 2007. Development of high voltage vacuum circuit breakers in China. *IEEE Transaction on Plasma Science*, **35**(4):856-865. [doi:10.1109/TPS.2007.896929]

Martens, T., Nellis, G.F., Pfotenhauer, J., Jahns, T., 2005. Double-sided IPEM Cooling Using Miniature Heat Pipes, *IEEE Transactions on Components and Packaging Technologies*, **28**(4):852-861. [doi:10.1109/TCAPT.2005.848591]

Matsui, Y., Saitoh, H., Nagatake, K., Ichikawa, H., Sakaki, M., 2005. Development of Eco-friendly 72/84 kV Vacuum Circuit Breakers. Proceedings of International Symposium on Electrical Insulating Materials, Kitakyu-shu, Japan, **3**:679-682. [doi:10.1109/ISEIM.2005.193461]

Matsukawa, M., Miura, Y., Kimura, T., Watanabe, K., Kubota, T., Kawashima, S., 1998. Design and model test of a water-cooled VCB for superconducting magnet power supplies. *Fusion Technology*, **34**(3):684-688.

Matsukawa, M., Miura, Y., Terakado, T., Kimura, T., 2000. Development of a Vacuum Switch Carrying a Continuous Current of 36 KA DC. IEEE 19th International

Symposium on Discharges and Electrical Insulation in Vacuum, Xi'an, China, **2**:415-418. [doi:10.1109/DEIV.2000.879015]

Okubo, H., 2006. Development of Electrical Insulation Techniques in Vacuum for Higher Voltage Vacuum Interrupters. IEEE 22th International Symposium on Discharges and Electrical Insulation in Vacuum, Matsue, Japan, p.7-12.

Renz, R., 2006. High Voltage Vacuum Interrupters; Technical and Physical Feasibility versus Economical Efficiency. Proceedings of 22nd International Symposium on Discharges and Electrical Insulation in Vacuum, Matsue, Japan, p.257-262. [doi:10.1109/DEIV.2006.357281]

Wang, J., 2006. 126 kV Vacuum Circuit Breaker Debuted in China. IEEE 22th International Symposium on Discharges and Electrical Insulation in Vacuum, Matsue, Japan, p.1-5.

Xie, H., Ali, A., Bhatia, R., 1998. The Use of Heat Pipes in Personal Computers. The Sixth Intersociety Conference on Thermal and Thermomechanical Phenomena in Electronic Systems, Seattle, American, p.442-448. [doi:10.1109/ITHERM.1998.689600]

Yamano, Y., Kobayashi, S., Matsukawa, M., 2002. Measurements and Analysis of Temperature Rise at Electrodes of a Vacuum Interrupter for High Current Applications. IEEE 20th International Symposium on Discharges and Electrical Insulation in Vacuum, Tours, France, p.419-422. [doi:10.1109/ISDEIV.2002.1027398]

Yanabu, S., 2006. Historical review of high voltage switchgear developments in the 20th centurary for power transmission and distribution system in Japan. *IEEE Transactions on Power Delivery*, **21**(2):659-664. [doi:10.1109/TPWRD.2005.861228]

Zaghdoudi, M., Teytu, A., 2000. Use of Heat Pipes for Avionics Cooling. Proceedings of 3rd Electronics Packaging Technology Conference, Singapore, p.425-430. [doi:10.1109/EPTC.2000.906411]